Cost-effective Bridge Decks for Improved Durability and Extended Service Life — Experimental Testing and Performance Analysis of a Corrugated Core Bridge Deck with Structural Adhesive Bonding

FINAL REPORT
June 2023

Submitted By:

Sougata Roy[1] , Sophia Pastore[2], Haider Sakban[3], and Amirali Najafi[4]

[1]Former Associate Research Professor, Department of Civil and Environmental Engineering, Rutgers University

[2]Former Graduate Student, Department of Civil and Environmental Engineering, Rutgers University

[3]Graduate Student, Department of Civil and Environmental Engineering, Rutgers University

[4]Research Associate, Center for Advanced Infrastructure and Transportation, Rutgers University

Center for Advanced Infrastructure and Transportation
Rutgers, The State University of New Jersey. 100 Brett Rd. Piscataway, NJ, 08854

External Project Manager
Richard Dunne, Greenman-Pedersen, Inc.

In cooperation with

Rutgers, The State University of New Jersey
And
New Jersey Department of Transportation
And
U.S. Department of Transportation
Federal Highway Administration

Disclaimer Statement

The contents of this report reflect the views of the authors, who are responsible for the facts and the accuracy of the information presented herein. This document is disseminated under the sponsorship of the Department of Transportation, University Transportation Centers Program, in the interest of information exchange. The U.S. Government assumes no liability for the contents or use thereof.

The Center for Advanced Infrastructure and Transportation (CAIT) is a Regional UTC Consortium led by Rutgers, The State University. Members of the consortium are Atlantic Cape Community College, Columbia University, Cornell University, New Jersey Institute of Technology, Polytechnic University of Puerto Rico, Princeton University, Rowan University, SUNY - Farmingdale State College, and SUNY - University at Buffalo. The Center is funded by the U.S. Department of Transportation.

1. Report No.	2. Government Accession No.	3. Recipient's Catalog No.
CAIT-UTC-REG28		

4. Title and Subtitle	5. Report Date
Cost-effective Bridge Decks for Improved Durability and Extended Service Life — Experimental Testing and Performance Analysis of a Corrugated Core Bridge Deck with Structural Adhesive Bonding	June 2023
	6. Performing Organization Code CAIT/Rutgers

7. Author(s)	8. Performing Organization Report No.
Sougata Roy (https://orcid.org/0000-0001-8866-3076) Sophia Pastore (https://orcid.org/0009-0005-2831-3644) Haider Sakban (https://orcid.org/0000-0002-6947-6424) Amirali Najafi (https://orcid.org/0000-0002-7845-0859)	CAIT-UTC-REG28

9. Performing Organization Name and Address	10. Work Unit No.
CAIT, Rutgers Rm 224, 100 Brett Rd. Piscataway, NJ, 08854	11. Contract or Grant No. 69A3551847102

12. Sponsoring Agency Name and Address	13. Type of Report and Period Covered
Center for Advanced Infrastructure and Transportation Rutgers, The State University of New Jersey 100 Brett Road Piscataway, NJ 08854	Final Report 12/01/2019-03/31/2023
	14. Sponsoring Agency Code

15. Supplementary Notes
U.S. Department of Transportation/OST-R
1200 New Jersey Avenue, SE
Washington, DC 20590-0001

16. Abstract

This project involves experimental testing of a novel bridge deck with a corrugated core that is bonded to the deck plate using structural adhesive. The specimen was supported and loaded using specially designed fixtures. Comprehensive instrumentation was implemented, including uniaxial, biaxial, and rosette strain gauges, as well as displacement transducers. The testing program comprised initial static tests, fatigue tests, and intermittent static tests. The fatigue test was conducted for 5 million cycles. Analysis of the static test results suggested degradation of the adhesive connection between the core and the deck plate due to fatigue loading, leading to changes in transverse load distribution and decreased deck stiffness. However, the structural integrity of the deck was not compromised. This study showed the potential for cost-effective fabrication of steel sandwich plate decks using structural adhesive.

17. Key Words	18. Distribution Statement
Corrugated Core, Bridge Deck, Structural Adhesive, Adhesive Connection, Steel Sandwich Plate Deck, Fatigue Test, Static Test	

19. Security Classification (of this report)	20. Security Classification (of this page)	21. No. of Pages	22. Price
Unclassified	Unclassified	33	

Form DOT F 1700.7 (8-69)

ACKNOWLEDGEMENTS

The research presented in this report was partially sponsored by a grant received from the United States Department of Transportation, University Transportation Centers Program. The first author Dr. Sougata Roy, served as the Principal Investigator for this project. The research contributed to the project report for fulfillment of master's degree requirements of Ms. Sophia Pastore. Mr. Haider Sakban assisted with the experimental setup and fatigue testing. Dr. Amirali Najafi collated and assisted with the review of the report. The authors gratefully acknowledge the support received for this study, particularly the help with procurement of the servo hydraulic testing equipment. Special thanks are due to Dr. John Braley, Research Associate of Rutgers CAIT for helping with instrumentation and data acquisition Special thanks are also due to Mr. Richard Dunne of GPI Inc for valuable technical feedback. Finally, the authors would like to thank Mr. Patrick Szary, Ms. Marta Zubriggen, and Mr. Ryan Stiesi of Rutgers CAIT for the administrative support.

TABLE OF CONTENTS

LIST OF FIGURES

1. PROBLEM DESCRIPTION

Deterioration of decks over time is a major challenge for the durability of highway bridges in the United States. These bridges experience continuous wear and tear from vehicular traffic, weather conditions, and winter de-icing agents, leading to the degradation of concrete bridge decks. Although traditional reinforced concrete decks are commonly used due to their lower initial cost, they are prone to corrosion damage, necessitating frequent repairs or replacements (Nemry et al., 2012). This reduces the useful service life of the bridge infrastructure and increases the overall cost of the bridge over its lifecycle.

The maintenance costs associated with deck repairs, along with the time and resources required for traffic diversion and operation during repairs, further strain the already limited infrastructure budget and negatively impact the nation's economy. Moreover, many bridges in the aging U.S. bridge inventory have inadequate design strength to meet operational ratings or cannot support thicker concrete decks to accommodate heavier truck loads. This necessitates reducing the deadload of the superstructure.

The identified problems highlight the need for comprehensive solutions that can mitigate the financial cost on infrastructure budgets and minimize disruptions to traffic flow during repair activities. To address the challenges, a cost-effective alternative is being developed, which is a steel bridge deck known as a steel sandwich plate (SSP) deck. This innovative deck design has similar stiffness to concrete decks but is lighter in weight, allowing for rapid construction and demonstrating improved durability and extended service life. However, fabrication of this deck, particularly joining the outer plates with the core by traditional welding is a challenge. Adhesive bonding of steel corrugated core sandwich structures is a viable option and offers several advantages compared to traditional fabrication methods, particularly with respect to fabrication efficiency and fatigue loading on connections (Knox et al., 1998). In this project, one such deck design was investigated for structural performance. Laboratory testing of the novel SSP deck, which consisted of a corrugated core sandwiched between a top and bottom plate, where the top plate was bonded to the corrugated core using a structural adhesive instead of welding, is reported here. The objectives of this project were:

(1) to create a test setup in the Civil Engineering Laboratory (CEL) at Rutgers University specifically designed for testing the SSP bridge deck specimen,

(2) to conduct both static and fatigue tests on the specimen, and

(3) to evaluate the performance of the adhesive connection by analyzing the results obtained from the fatigue and static tests.

2. METHODOLOGY AND EXPERIMENTAL PROCEDURES

To achieve the project objectives, an experimental setup involving hydraulic actuator with 55 kips capacity supported by steel reaction frame fixture was prepared to apply the static and fatigue loads on the steel bridge deck specimen. These fixtures were specifically tailored for the project and designed to be reusable for future specimens of different sizes. The SSP deck specimen was 8' × 4'-3". The specimen was instrumented with various types of strain gauges (uniaxial, biaxial, and

rosette) as well as displacement transducers. The response data was recorded using a data acquisition system. The test program consisted of initial static testing, fatigue testing, and intermittent static testing during the fatigue testing phase, which lasted for 5 million cycles. Data was continuously collected throughout the test program. Finally, the static test results were analyzed to examine any changes in the specimen and evaluate the performance of the adhesive connections under fatigue loading.

2.1. Experimental Setup

2.1.1. Specimen Description

The bridge deck specimen was 4'-3" (130 cm) wide and 8' (244 cm) long. It featured a corrugated core, which was welded to the bottom plate at the valleys of the corrugation. Additionally, the corrugated core was bonded to the top plate using adhesive. Vertical plates were welded to both the top and bottom plates at the sides and ends of the specimen. Figure 1 depicts the details of the bridge deck and its components.

2.1.2. Test Fixture

The deck testing was planned to replicate its primary one-way behavior in the transverse direction, which was perpendicular to the corrugations. To achieve this, the deck was supported along its two longitudinal edges. The objective was to assess the deck's performance when subjected to the influence of a single tire contact area measuring 10" x 20" (25.4 cm X 50.8 cm), positioned at the middle span. This specific tire contact area is recommended by the AASHTO LRFD Bridge Design Specifications (LRFD BDS). A 55-kip Mechanical Testing Systems (MTS) servo-hydraulic actuator was utilized to apply the load to the specimen, reacting against an overhead frame and transmitting through a loading pad.

The CEL floor was equipped with threaded holes arranged in a grid pattern, with a spacing of 2'-3" (68.6cm) in one direction and 2'-6" (76.2 cm) in the other. The test fixtures were specifically designed to be bolted to the floor

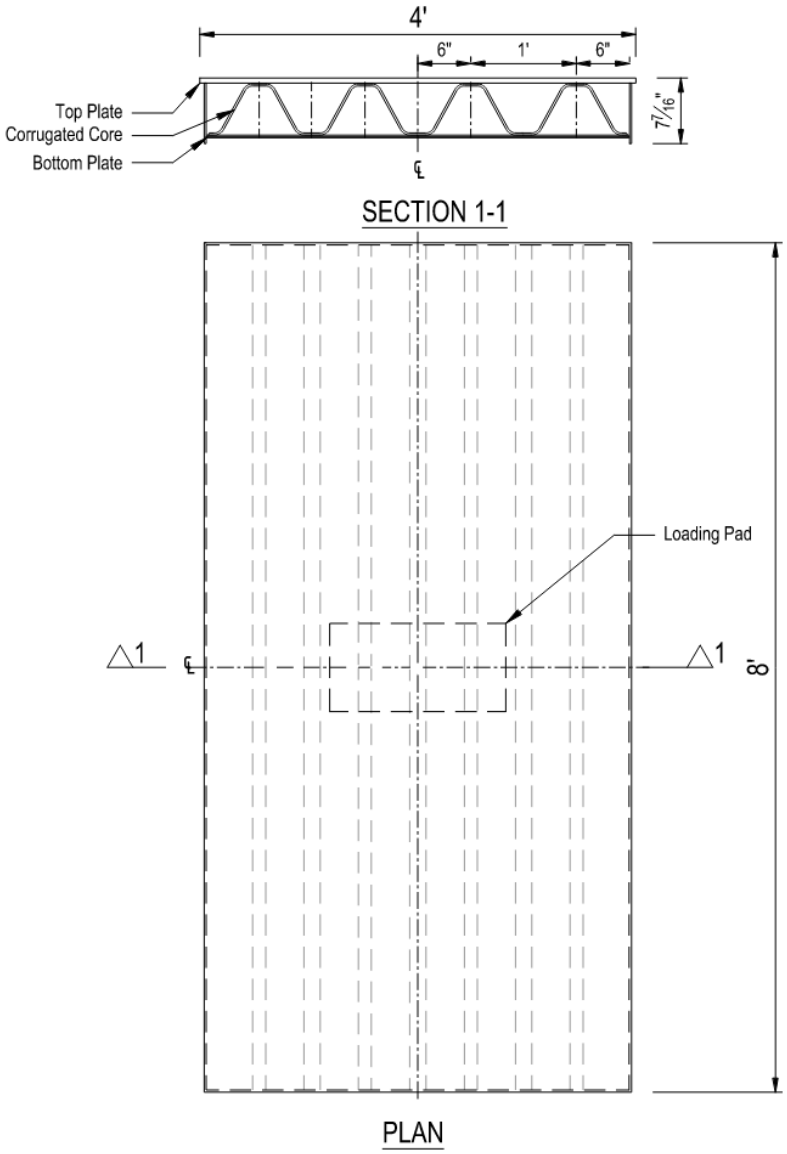

Figure 1 Plan and cross-sectional views of the bridge deck specimen. (1inch =2.54 cm)

Out of the three actuators (22.5 kip, 55 kip, and 110 kip capacity) procured by CEL, the 55 kip actuator was utilized for load application on the deck specimen. The 55 kip actuator was connected to the MTS hydraulic pump having a flow rate of 30 gpm at 3000 psi working pressure. The actuator was controlled remotely using the accompanying control software.

All the test fixtures were fabricated out of steel sections. The fixture supporting the specimen consisted of three columns on each longitudinal side of the specimen, positioned at the ends and center, with a beam spanning across the columns. The columns were designed with base plates and bolted down to the laboratory floor. Cap plates were also incorporated into the column design, and the beams were bolted to the column cap plates. Figure 2 illustrates the test arrangement and fixtures used in the experimental setup.

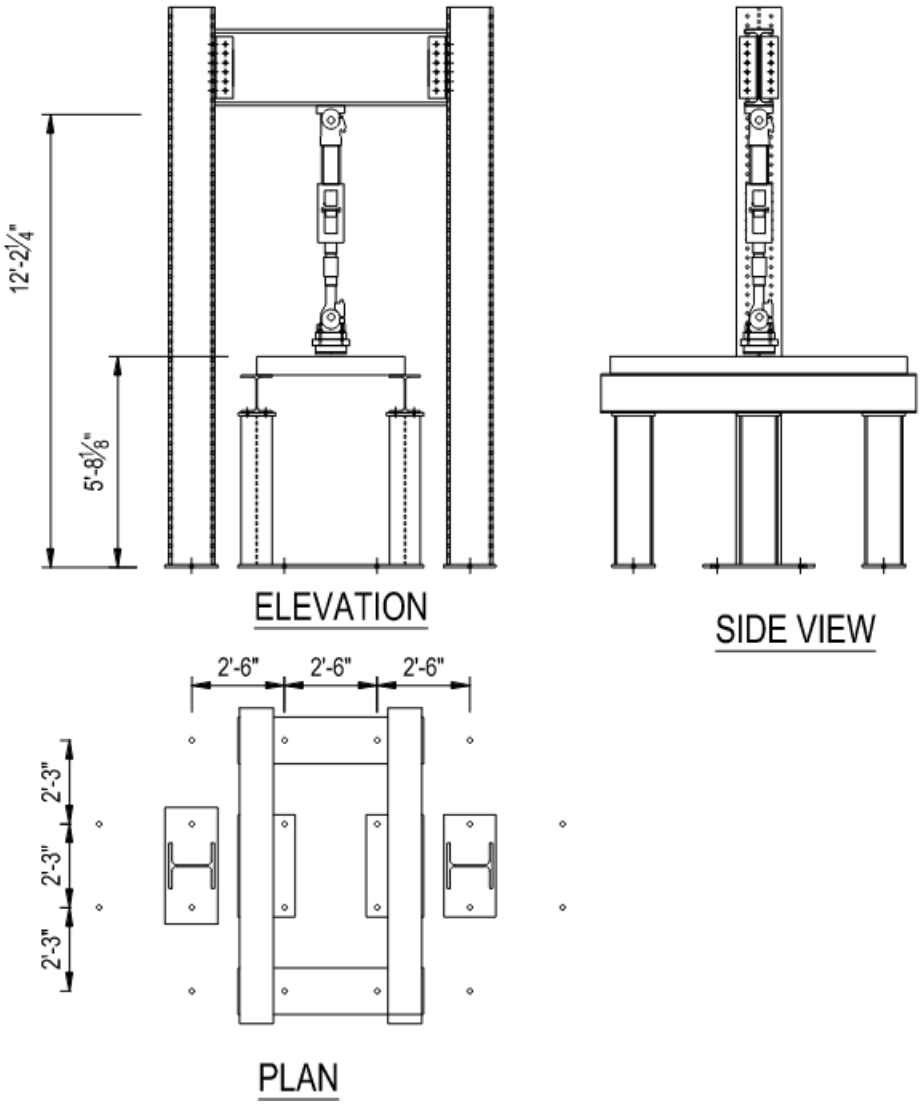

Figure 2 Elevation, side view, and plan view of support fixtures (1inch =2.54 cm)

To support the actuator, an overhead portal frame was installed in the transverse direction of the specimen. The frame columns were equipped with base plates for attaching to the floor. The actuator itself was bolted to the lower flange of the frame beam.

The test fixtures in the laboratory were assembled in the following sequence. The deck supports were installed first, followed by the the loading frame. Next, the deck specimen was positioned in place. Finally, the actuator was installed, followed by the loading pad.

To ensure uniform distribution of the load from the actuator onto the deck, a loading pad was employed. The LRFD BDS tire contact area was simulated using three 2-inch-thick plates arranged in a stack, with dimensions of 10”×20”. A rubber pad, 1/2” thick, was affixed to the bottom of the loading block. The bottom plate was provided with four threaded rods welded to its surface at the four corners, which extended through the other plates and finished with nuts at the top. The details of the loading pad are shown in Figure 3.

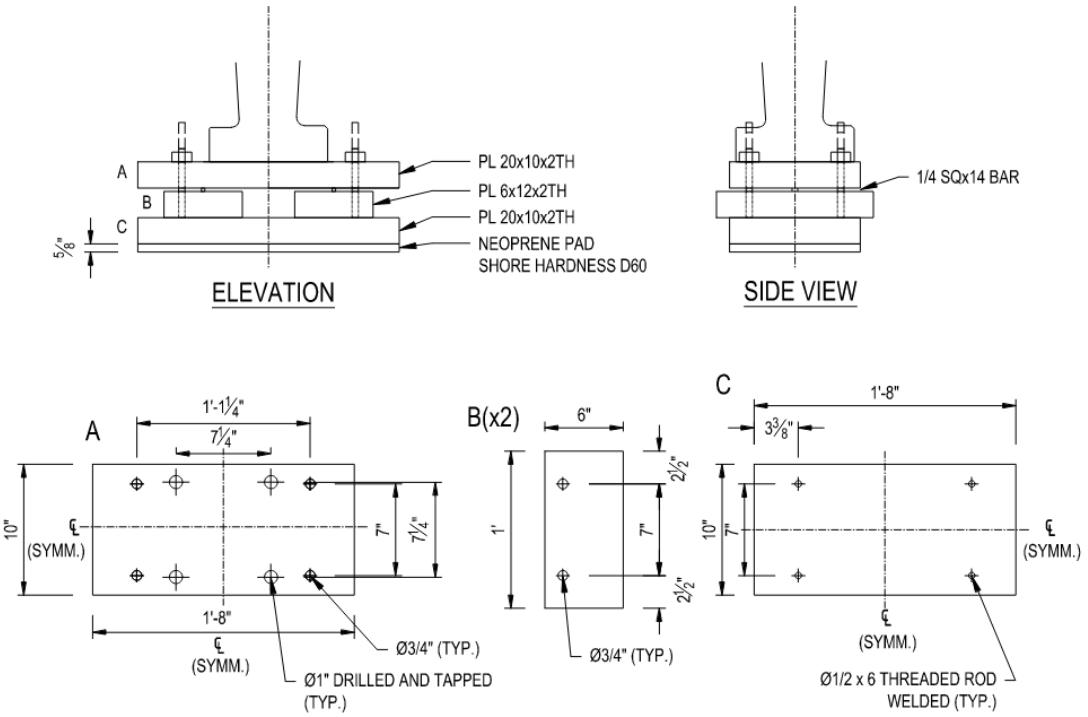

Figure 3 Details of loading pad (1inch =2.54 cm)

2.1.3. Test Fixture Adjustments

Significant bowing of the edge plates was noted in the deck specimen as delivered, resulting in the specimen being primarily supported at the corners. Additionally, distortion of the supporting beam top flange led to partial support at the longitudinal edge, which deviated from the intended boundary condition. Shims were strategically placed along the longitudinal edges to ensure support solely by the edge plates onto the support beams. Figure 4 and Figure 5 illustrate the deck after the shims were added, highlighting the previous contact area. Furthermore, large C-clamps were affixed to the corners and center of the deck on both sides to prevent any movement during cyclic testing. A fence, fabricated out of welded angle pieces, was placed around the loading pad and clamped to the deck plate edge, to prevent the loading pad from “walking” out of position (Figure 6). The actuator was restrained in alignment by an angle member bolted to the back of the actuator and to the loading frame columns (Figure 7). Out of plane rocking of the loading frame during cyclic loading was braced by heavy duty pretensioned chains bolted to the loading frame and to the laboratory floor.

Figure 4 Shims to support deck edge

Figure 5 Straight-on view of shims

Figure 6 Loading pad with fence around

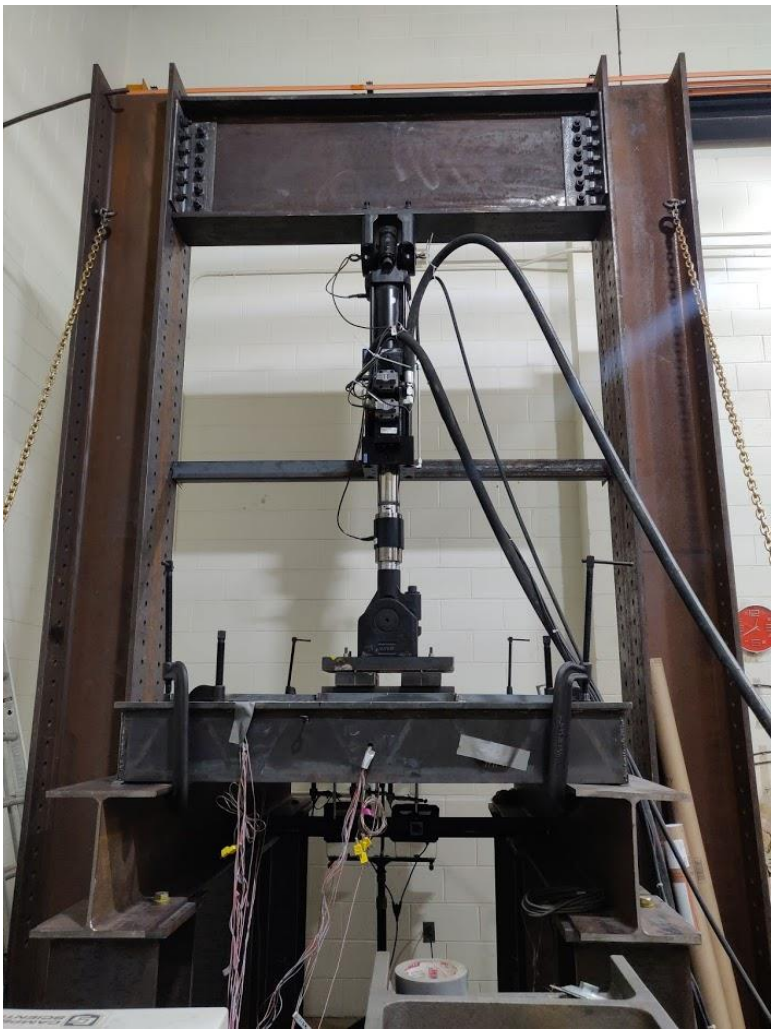

Figure 7 Overall test setup – end view

2.2. Specimen Instrumentation

A comprehensive instrumentation plan was developed for the deck. Critical locations and values for strains and displacement within the deck were assessed in view of the one way spanning of the deck specimen in the transverse direction. The critical strains and displacements within the deck were determined to be at the midspan section, specifically under the load and perpendicular to the corrugations. The response in the corrugations near the top and bottom junctions with the plates and the interface shear between the corrugations and the plates were of interest. Furthermore, biaxial strain response was expected in the deck plates under the load.

Considering geometric and loading symmetry, strain gauges were positioned on only one side of the deck. The instrumentation included electrical resistance foil strain gauges and linear voltage differential transformers or LVDTs as displacement transducers.

2.2.1. Strain Gauges

A total of eight strain gauges were installed, including one uniaxial gauge, two biaxial gauges, and five rectangular rosette gauges. This installation resulted in a total of 20 channels for data collection. The placement of the rosette gauges aimed to capture the complex strain fields at the connections between the corrugations and the outer plates. Specifically, the two 90-degree arms of the rosette gauges were oriented along the longitudinal direction of the deck and the transverse direction along the corrugation face.

The biaxial gauges were strategically positioned on the top and bottom plates, primarily in areas where significant biaxial strains were expected, such as under the load pad. Two biaxial gauges were placed on the top plate, with one on the top face and the other on the bottom face, configured in a back-to-back arrangement. The arms of the biaxial gauges were aligned with the longitudinal and transverse directions of the deck.

The uniaxial gauge was installed on the underside of the bottom plate at the midspan location, oriented in the longitudinal direction. Detailed plans for the gauge placements can be seen in Figure 8 and Figure 9.

A naming convention was established for the strain gauges, consisting of the format C#/DP/BP_S/N_T/B_U/B/R#. The first term denoted the element of the deck being gauged, namely "C#" representing the corrugation (e.g., "C1," "C2"), "DP" indicating the deck plate, and "BP" referring to the bottom plate. The second term identified the side of the corrugation, either "S" for South or "N" for North, with respect to the longitudinal East-West orientation of the specimen in the laboratory. The third term described the gauge location as either "B" for the bottom or "T" for the top of the component. The last term represented the type of gauge, with "B" for biaxial, "U" for uniaxial, and "R" for rosette gauges, followed by the channel number. For instance, the designation "C1_S_T_R1" referred to one arm of a rosette gauge installed on the south side the top end of corrugation C1. Strain gauges located internally within the deck, such as: C1_S_T_R1,2,3; C1_S_B_B4,5; C2_N_T_R6,7,8; C2_S_T_R9,10,11; and DP_B_B12,13, were installed at the fabricator's facility before the outer plates were installed. The rosette gauges on the corrugations were installed as close to the peaks and valleys as

possible, without encroaching on the corner fillets (Figure 10). The other three gauges were installed on the top of the deck plate and on the underside of the bottom plate. These gauges were installed in the laboratory. The strain gauge DP_T_R14,15,16 was installed on the top of the deck plate at the longitudinal and transverse center of the deck, directly under the loading pad. The strain gauge BP_B_R17,18,19 was installed on the underside of the bottom plate, below the north side of the corrugation C2 along the transverse centerline of the deck. Lastly, the strain gauge BP_B_U20 was installed on the underside of the bottom plate at the center of the deck, in

line with BP_B_R17,18,19 in the transverse direction.

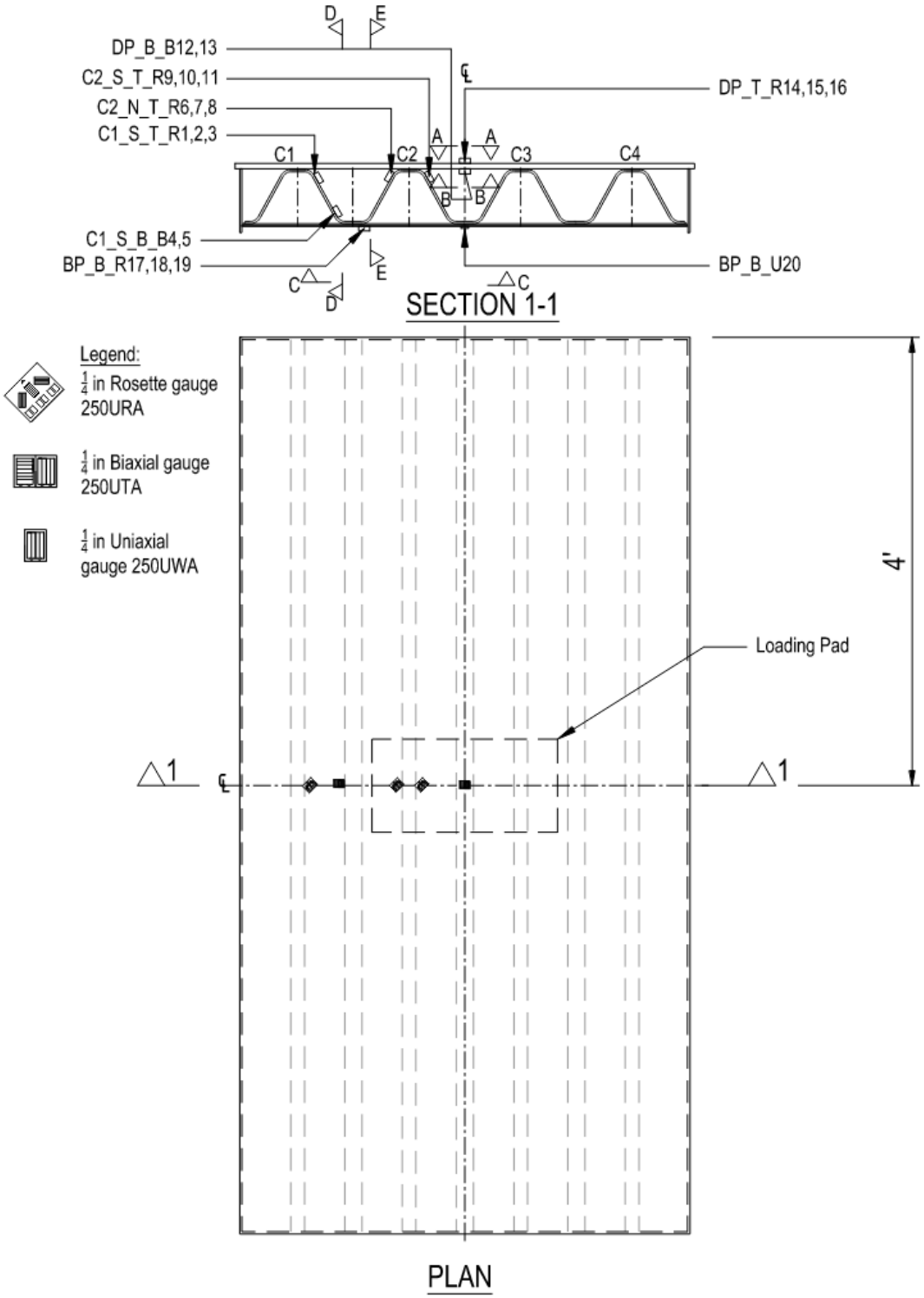

Figure 8 Plan and cross sectional view of strain gauge layout

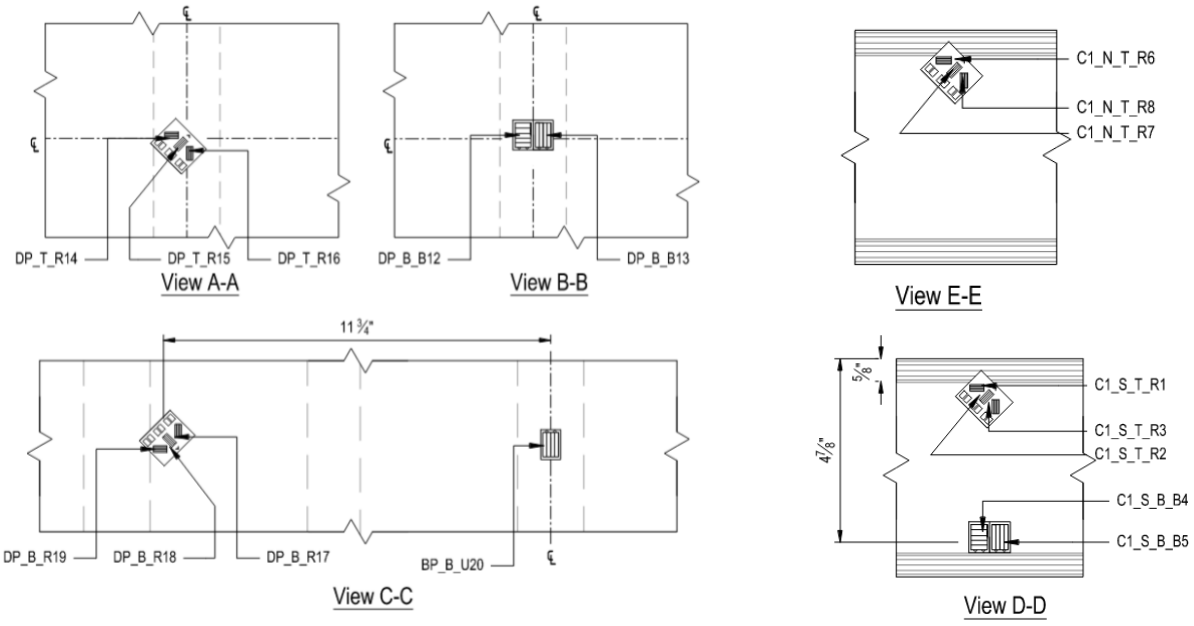

Figure 9 Close up views of strain gauge layout showing orientation of gauges

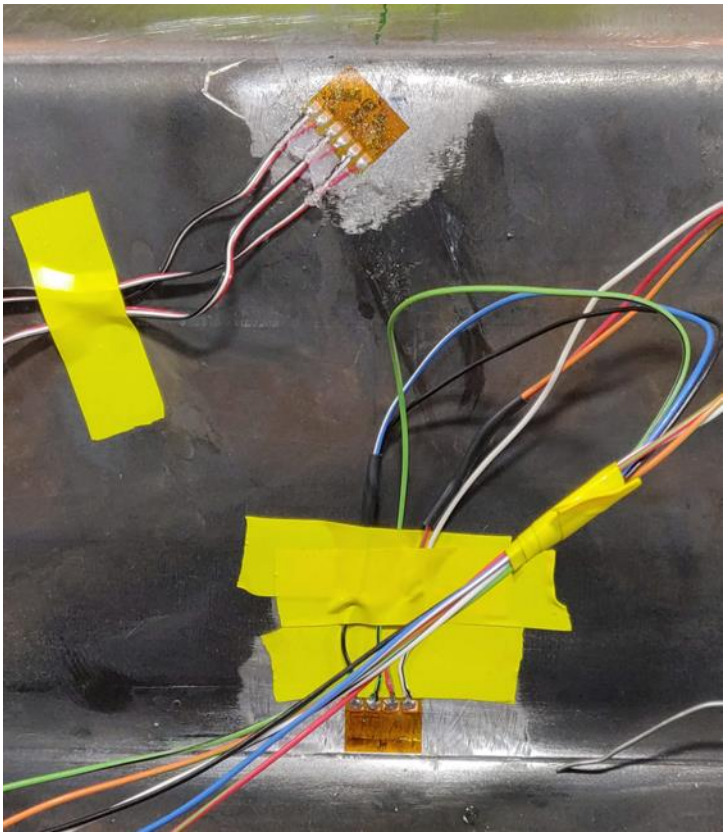

Figure 10 Close up of internal stain gauges on corrugation with connected wires

Electrical resistance foil type bondable strain gauges from Micro-Measurements were used. . The uniaxial strain gauge was CEA-06-250UWA-350, while the biaxial gauges were CEA-06-250UTA-350. The rosette gauges were CEA-06-250URA-350. These are general purpose strain gauges for use on steel having a resistance of 350Ω. The gauge length was 0.250", with an overall length of 0.450" for the uniaxial and biaxial gauges, and 0.50" for the rosette gauges. Wiring was facilitated through the exposed solder tabs on the gauges.

The strain gauges were designed to operate safely within a temperature range of -100°F to 350°F. The adhesive connection between the deck plate and the corrugation underwent heat curing above 275°F, which was within the safe operating temperature range for the gauges. However, it is important to note that the glue used to bond the gauges to the deck had a safe operating temperature of approximately 200°F. The utilization of an alternative epoxy-based glue was not feasible due to challenges related to heat curing the glue for a relatively large component, as well as difficulties in applying the required pressure. Consequently, while the strain gauges themselves were unaffected by the heat curing process during fabrication of the deck (deck plate-to-corrugation connection), the glue used to bond them to the deck plate may have been impacted.

2.2.2. Displacement Sensors

Linear variable differential transformers (LVDTs) were employed as displacement transducers to measure the vertical deflection of the deck at the midspan section during static tests. Considering the symmetry of the deck, three LVDTs were positioned on one side of the specimen in the transverse direction, as shown in Figure 11.

Magnetic clamps were utilized to install the LVDTs, which were affixed to an angle member in the transverse direction and connected to the middle column supports. The precise location of the LVDTs was adjusted to avoid interference with the strain gauges on the deck soffit. Consequently, the LVDTs were placed at a quarter inch offset from the center line, all positioned on the same transverse section (See Figure 12). During fatigue testing, the LVDTs were removed as they would not have yielded meaningful information .

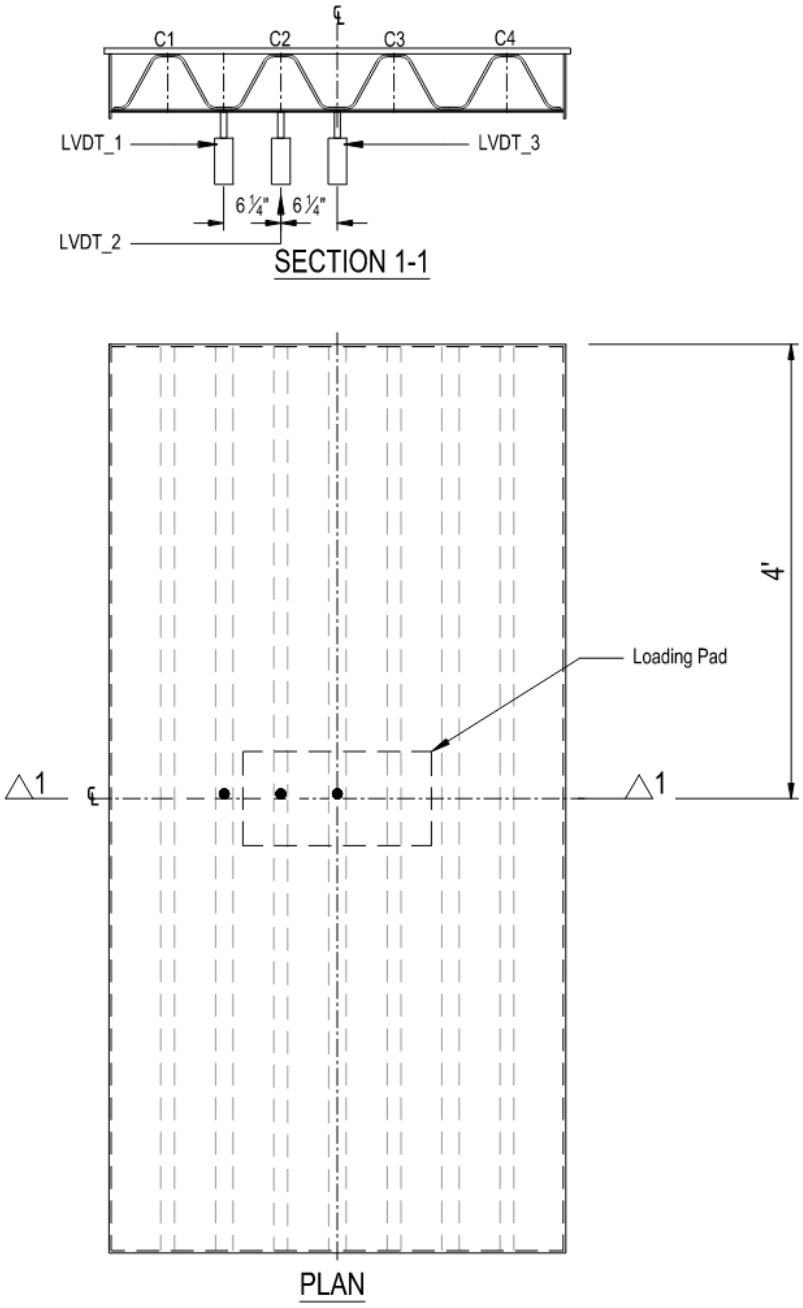

Figure 11 Plan and cross sectional view of LVDT layout

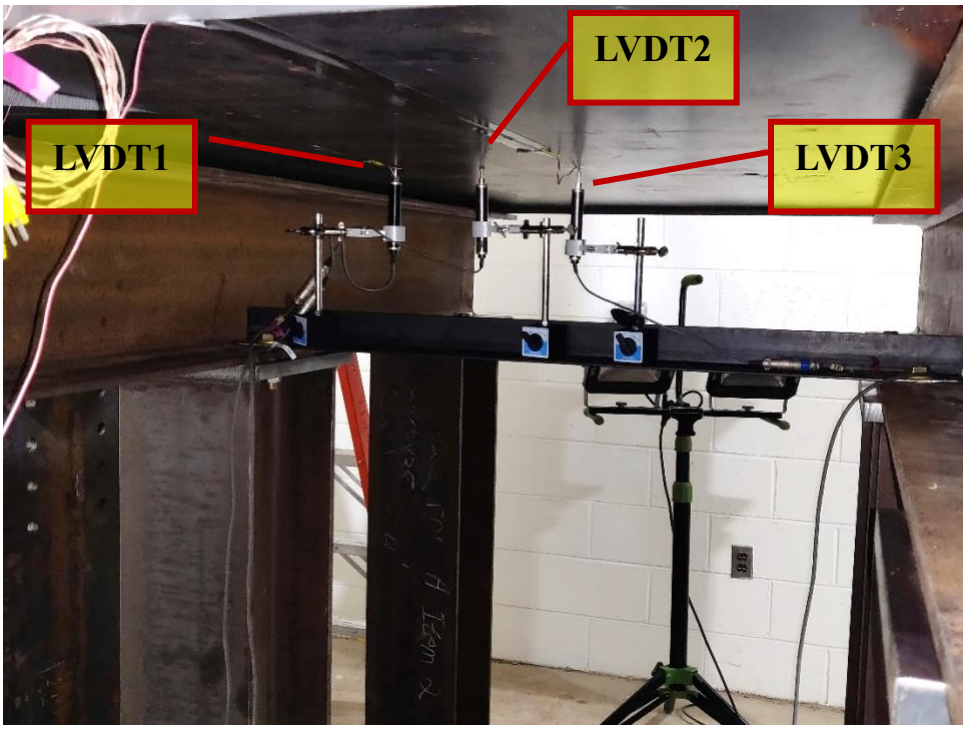

Figure 12 LVDT installation in the lab

2.2.3. Data Acquisition

The data from the strain gauges and LVDTs were collected by a Campbell Scientific CR1000X data logger, which was equipped with a CDM-A116 expansion module for accommodating all the channels (See Figure 13). Additionally, the load signal from the actuator controller was collected at the data logger to ensure synchronization of the measurements with the applied load.

During the static testing phase, the strain data from the gauges and the displacement measurements from the LVDTs were continuously recorded throughout the entire test. The data logging process involved capturing data 10 times per second for a duration of 110 seconds, as the actuator progressively applied load from 0 kip to a peak and back to 0 kip. As a result, a total of 1,100 data points were generated per static test per data channel.

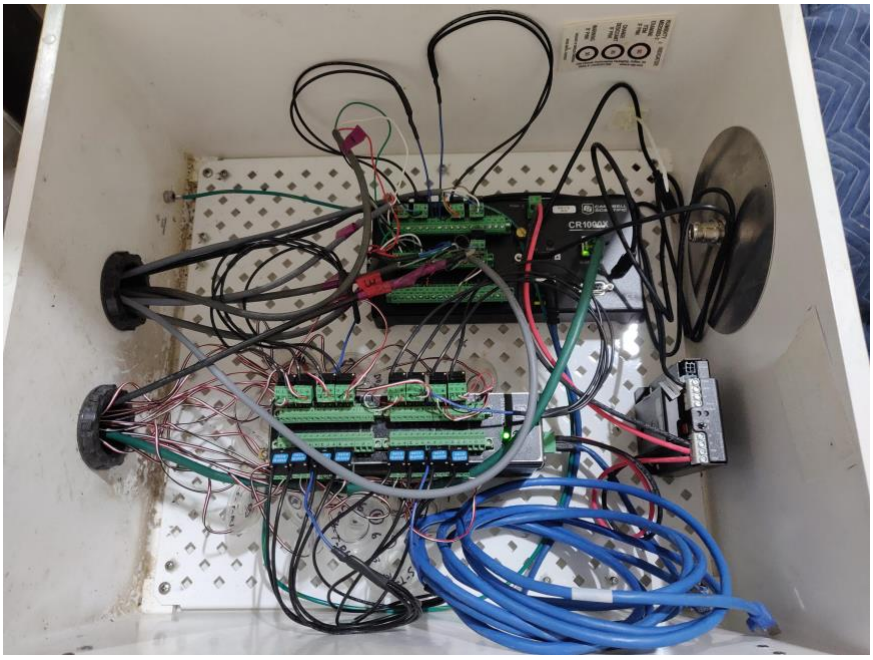

Figure 13 CR1000X and CDM-A116 data loggers

2.3. Testing

2.3.1. Procedure

The specimen was tested for both static and fatigue (cyclic) loading. Initially, a static test was conducted to establish the pristine condition of the structure and to determine the loading for fatigue testing. Throughout fatigue testing, periodic static tests were performed to monitor any change in the structural condition. These tests were conducted during the third, fourth, and fifth weeks of testing, specifically at approximately 3, 4, and 5 million cycles. The number of cycles was recorded by both the controller and the data logger, with slight variations between the two measurements. The total cycle counts were 5,025,270 and 5,013,897, respectively, resulting in a difference of 0.23%.

2.3.2. Loading

The loading pattern for the static test followed a stepped pattern shown in Figure 14. The loading profile for the static test was as follows: monotonically load the actuator to 2 kips in 10 seconds; hold for 10 seconds; monotonically increase to 26.0 kips in 30 seconds; hold for 10 seconds;, monotonically decrease to 2 kips; hold for 10 seconds; and finally unload the actuator.

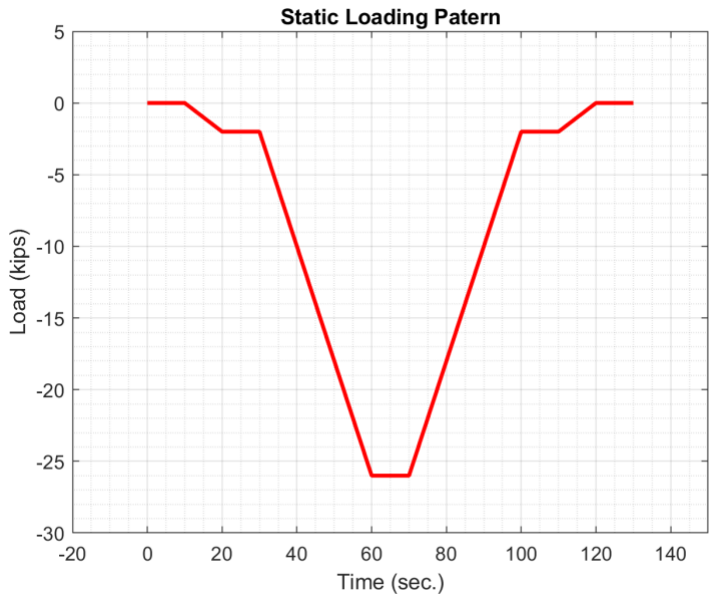

Figure 14 Static Loading Pattern

The minimum and maximum load for the fatigue test were also set as 2 and 26 kips, respectively. The fatigue testing was carried out under sinusoidal loading at a frequency of 2 Hz, as illustrated inFigure 15 Fatigue Loading Pattern for a 10 second interval. The fatigue test was conducted around the clock, except for routine maintenance. Throughout the testing period, the fatigue test was inspected and monitored five times each day, or approximately every 30,000 cycles (or 60,000 cycles overnight).

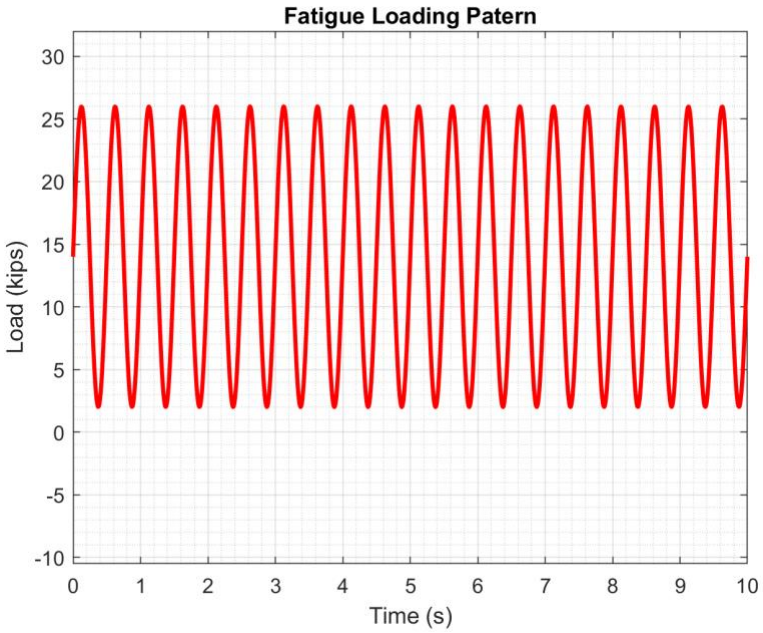

Figure 15 Fatigue Loading Pattern

3. TEST RESULTS AND DISCUSSION

The performance of the deck specimen subject to cyclic loading was assessed by comparing the results of the static and fatigue tests conducted at the initiation of fatigue testing and intermittently during the fatigue test. The test results are presented as sensor response vs applied load, with the applied load plotted on the abscissa and the sensor response plotted on the ordinate. Three static tests were performed on May 17, at the start of the fatigue test, on June 4, after 3 million fatigue cycles and on June 16, 2021, at the conclusion of the fatigue test after 5 million cycles. Stress is shown as the result of the strain gauge observations. For the purpose of converting measured strains to stresses, an assumed universally recognized modulus of elasticity (E) of 29,000 ksi and Poisson's ratio (ν) of 0.3 were used. The static test data from each date has been displayed using the same color, line type, and symbols for uniformity and simplicity of comparison. The sensor ID and the test date in m/d format are included in the legend for each plot.

3.1. Measurements by the Uniaxial Gauge

Figure 16 shows the static and the fatigue test measurements made by the uniaxial strain gauge BP_B_U20, which was positioned in the middle of the deck on the underside of the bottom plate and was oriented in the longitudinal direction of the specimen. This gauge was provided to measure the longitudinal flexural stresses at the soffit of the deck.

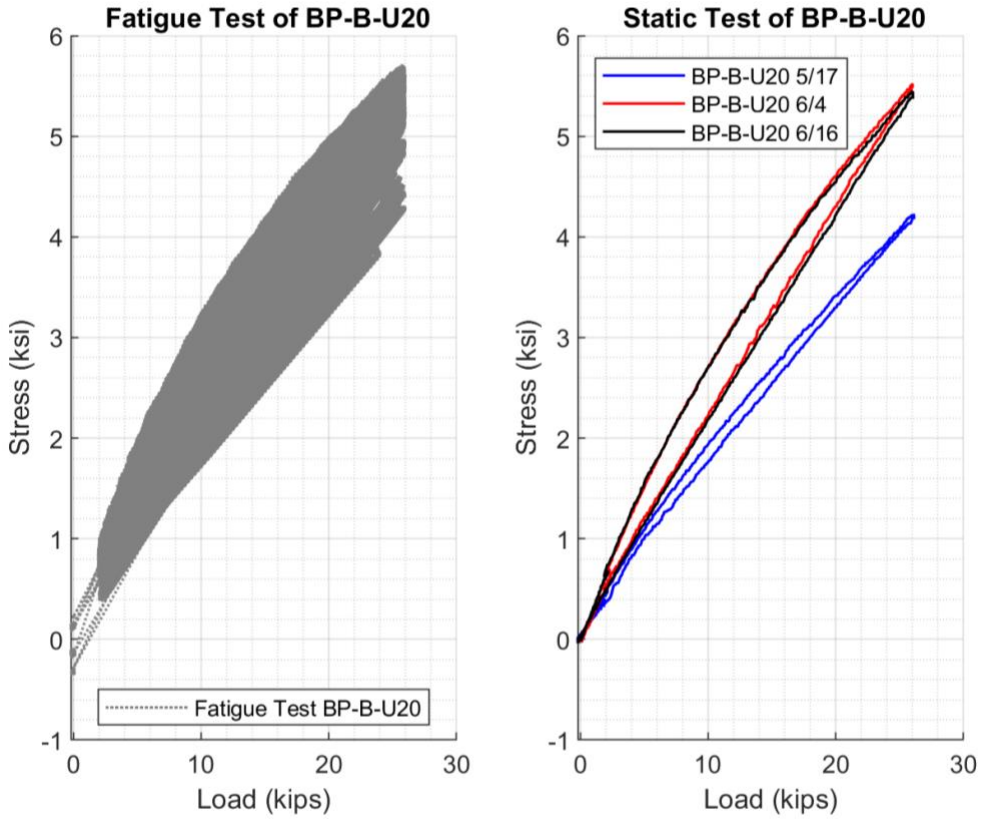

Figure 16 Fatigue and static test results of BP_B_U20

The strain gauges exhibited a slight deviation from linearity and displayed hysteresis in their response. This non-linear hysteretic behavior raises concerns regarding the integrity of the adhesive bond between the deck plate and the corrugated core. The deck was supported in a way that caused the main response in the transverse direction. As the fatigue testing progressed, the longitudinal stress response of the deck increased, indicating a potential compromise in the transverse load transfer within the deck. This deterioration was likely attributed to the weakening of the adhesive bond between the core and the deck plate. However, it is worth noting that the response eventually stabilized, as demonstrated by the nearly identical results observed in the second and third static tests.

3.2. Measurements by the Biaxial Gauges

Figure 17 presents the measurements obtained from the biaxial gauge positioned at the center of the deck, on the underside of the top plate. The gauge arms, labeled as B12 and B13, were aligned in the transverse and longitudinal directions, respectively.

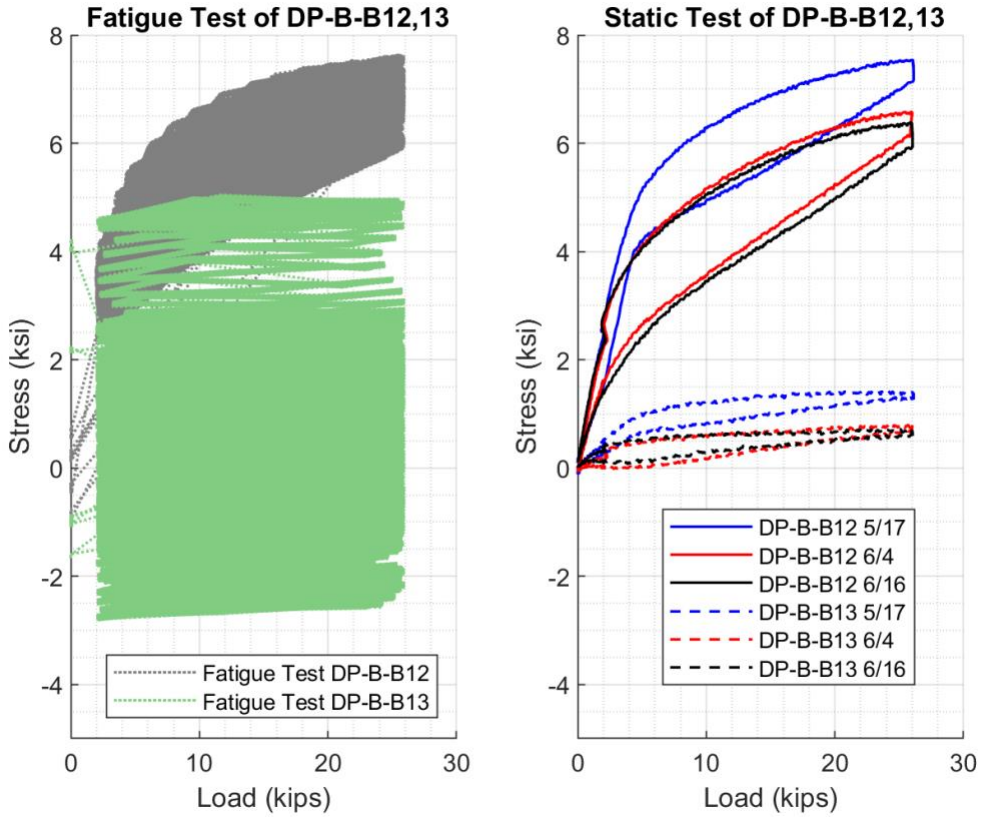

Figure 17 Fatigue and static test results of DP_B_B12,13

The gauge displayed a significant nonlinear and hysteretic response. In both directions, the measurements from the first test (5/17) were significantly higher than those from the other two tests (6/4 and 6/16). This suggests that between one and three million cycles of testing, the condition of the deck changed significantly. While the significant nonlinear and hysteretic behavior could be due to the behavior of the adhesive connection between the corrugated core and the deck

plate, the performance of the strain gauge is also in doubt. A cyanoacrylic glue, with an operating temperature of approximately 200°F, was used to attach the strain gauge to the deck plate prior to its attachment to the core. The adhesive connection between the deck plate and the core was heat cured at temperatures above 275°F after the installation of the deck plate. This exposure to high temperatures likely impacted the bond between the strain gauge and the deck plate, resulting in the observed response. However, the non-linear and hysteresis behavior observed in the uniaxial gauge installed on the soffit of the deck after the fabricated deck was installed in the laboratory indicates that some of this behavior can be attributed to the adhesive connection between the deck plate and the core. Nevertheless, the gauge response remained consistent across three trials for each test and between the tests conducted after 3 and 5 million cycles. The deck plate primarily experienced loading in the transverse direction, spanning between the crest of the corrugations, as evidenced by the higher response of the biaxial gauge arm in the transverse direction.

Figure 18 displays the biaxial gauge C1_S_B_B4,5 positioned at the lower end of the southern slope of the first corrugation in the deck, situated north of the deck centerline. The gauge arm B5 was aligned with the incline (the transverse direction), while the gauge arm B4 was aligned with the longitudinal direction of the deck.

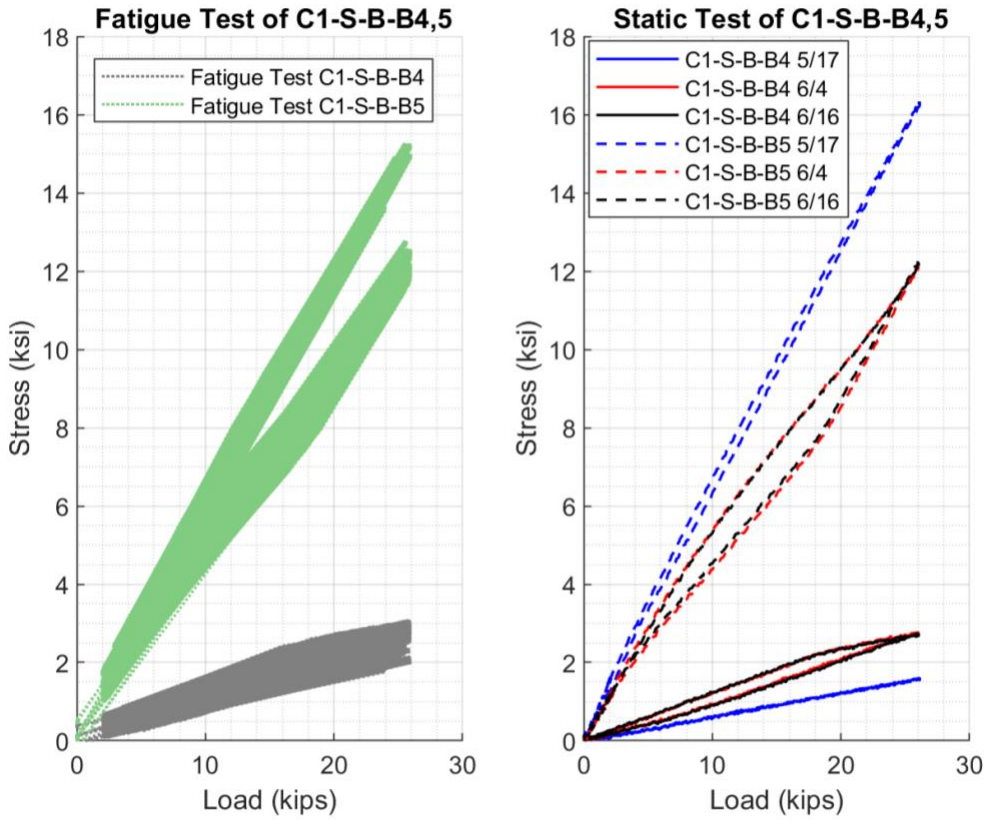

Figure 18 Fatigue and static test results of C1_S_B_B4,5

The response of gauge C1_S_B_B4 remained consistent and linear across the first static test and then the stress increased with a sign of nonlinear response. On the other hand, gauge B5 initially displayed primarily linear behavior with a slight presence of hysteresis during the first static test.

In subsequent static tests, the response of B5 remained mostly linear but reduced significantly, with consistent results observed between the tests conducted after 3 and 5 million cycles in both gauges (B4 and B5). The hysteresis in the response also increased during these two tests. The response of this gauge also suggests a change in the deck condition during the 3 million cycles of fatigue testing. It is worth noting that this gauge was positioned near the welded connection between the core and the bottom plate and captured the stresses in the corrugation slope. The observed hysteresis in its response was likely due to the condition of the adhesive connection between the core and the deck plate. The decrease in gauge response and the increase in hysteresis can be attributed to the deterioration of the adhesive connection between the core and the top plate, resulting in a change in stiffness and reduced stress on the corrugations.

3.3. Measurements by the Rosette Gauges

Five rectangular rosette gauges were positioned on the deck, each featuring three arms arranged at 0, 45, and 90-degree angles. The installation of these gauges ensured that the perpendicular arms were aligned with the longitudinal and transverse orientations of the deck.

The gauge C1_S_T_R1,2,3 was positioned at the upper part of the first corrugation, located to the north of the deck centerline. Arm R1 was aligned with the longitudinal direction of the deck, while arm R3 was oriented in the transverse direction along the corrugation slope. Arm R2 was positioned at a 45-degree angle between R1 and R3. The measurements from this gauge are plotted in Figure 19.

The stresses experienced by this gauge were compressive throughout the test. The stresses along the slope of the corrugation (R3) were larger in magnitude compared to the stresses in the longitudinal direction of the deck, consistent with the predominantly one-way response of the deck in the transverse direction. The responses of R1 and R3 in the first static test were mostly linear and showed minimal hysteresis. However, as fatigue testing progressed, the response of R3 decreased significantly in magnitude and exhibited hysteresis. On the other hand, the response of R1 increased in magnitude without showing hysteresis. The response of the deck during static tests at 3 and 5 million cycles remained consistent, indicating that the deck condition changed during the 1 to 3 million cycles of testing. The decrease in response along the corrugation suggests a deterioration of the adhesive connection between the core and the deck plate during fatigue testing, affecting the transfer of transverse loads. However, this degradation seemed to stabilize after 3 million cycles of testing.

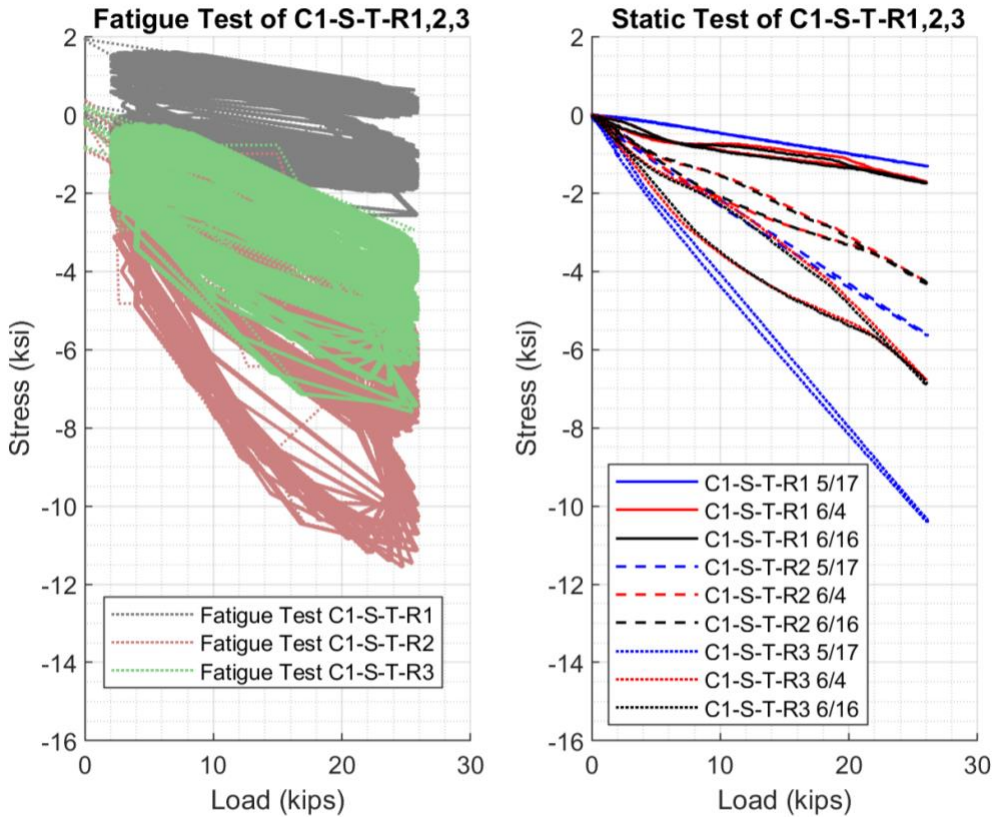

Figure 19 Fatigue and static test results of C1_S_T_R1,2,3

Figure 20 illustrates the response of the gauge C2_N_T_R6,7,8 positioned on the upper edge of the north side of the incline of corrugation C2, directly north of the deck center. Arm R6 was oriented in the longitudinal direction of the deck and arm R8 was oriented in the transverse direction along the incline of the corrugation. The arm R7 was situated at a 45-degree angle between R6 and R8.

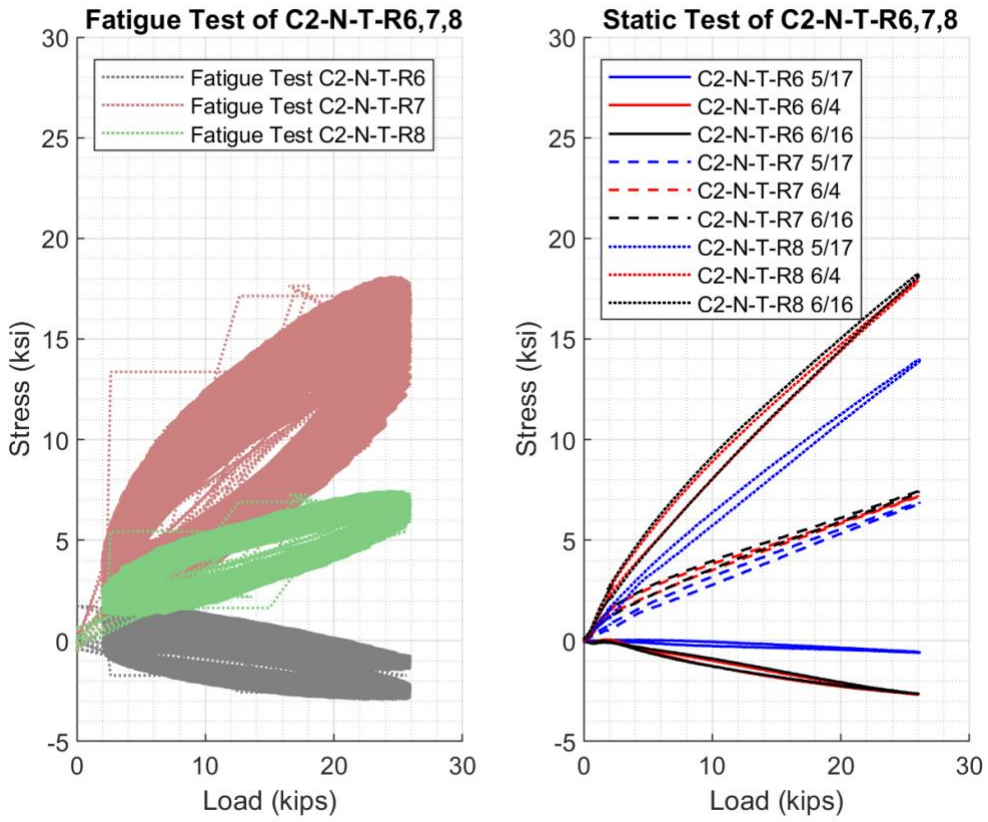

Figure 20 Fatigue and static test results of C2_N_T_R6,7,8

Arm R6, aligned with the longitudinal direction, exhibited compressive response, while arm R8, aligned with the transverse direction, showed tensile response. Overall, the gauge response, including all arms, was predominantly linear with slight nonlinearity observed during the initial 2 kip loading. The relatively smaller response of R6 indicated a greater strain experienced in the transverse direction. As the fatigue testing progressed to 3 million cycles, both responses increased in magnitude, indicating a deterioration of the adhesive connection between the core and the deck plate.

Figure 21 displays the response of gauge C2_S_T_R9,10,11. Positioned on the upper edge of the south side of corrugation C2 incline, it was directly opposite to C2_N_T_R6,7,8 on the north side. The gauge arm R9 was aligned with the longitudinal direction of the deck, R11 was oriented along the corrugation in the transverse direction, and R10 was positioned diagonally between the two arms.

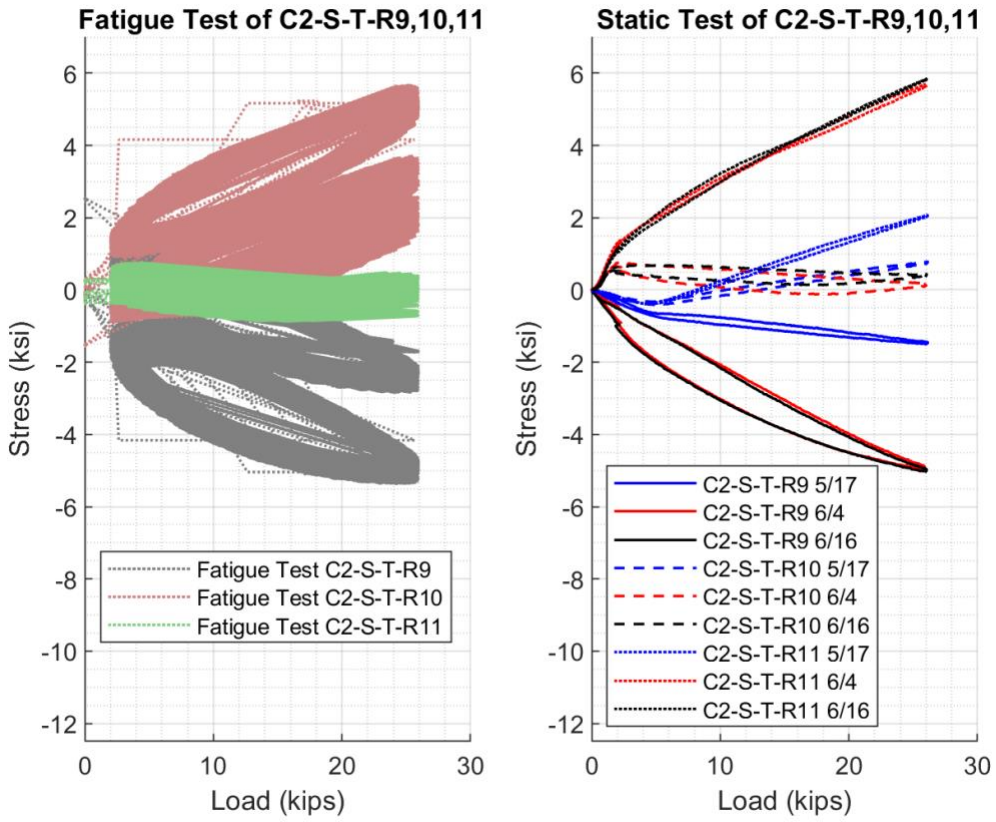

Figure 21 Fatigue and static test results of C2_S_T_R9,10,11

The strain gauge, with its R9 arm aligned longitudinally, displayed a compressive response, while the arm R11, aligned transversely, exhibited tensile response. Notably, the R11 arm achieved larger values compared to R9. Both arms exhibited hysteresis, particularly during the tests conducted on 6/4 and 6/16. Considering the configuration of the specimen, the gauges C2_S_T_R9,10,11 and C2_N_T_R6,7,8, should experience tensile and compressive stresses, respectively. However, the graphs show the opposite. The northern gauge is acting primarily in tension, and the southern gauge is acting primarily in compression. This could be due to local out-of-plane bending of the corrugated core. As the deck was loaded, the northern side of the corrugation stretched in tension, and the southern side was compressed. The stress on the southern side increased greatly between the initial test and the following tests. This suggests that more tension was experienced as the adhesive between the deck plate and the corrugation began to deteriorate. As the fatigue testing progressed to 3 million cycles, both responses increased in magnitude, suggesting a deterioration of the adhesive connection between the core and the deck plate.

Figure 22 illustrates the behavior of the gauge DP_T_R14,15,16. This gauge was positioned at the deck center on top of the top deck plate. Arm R14 was aligned in the transverse direction relative to the deck specimen, while arm R16 is oriented longitudinally. Additionally, arm R15 was situated diagonally between these two orientations.

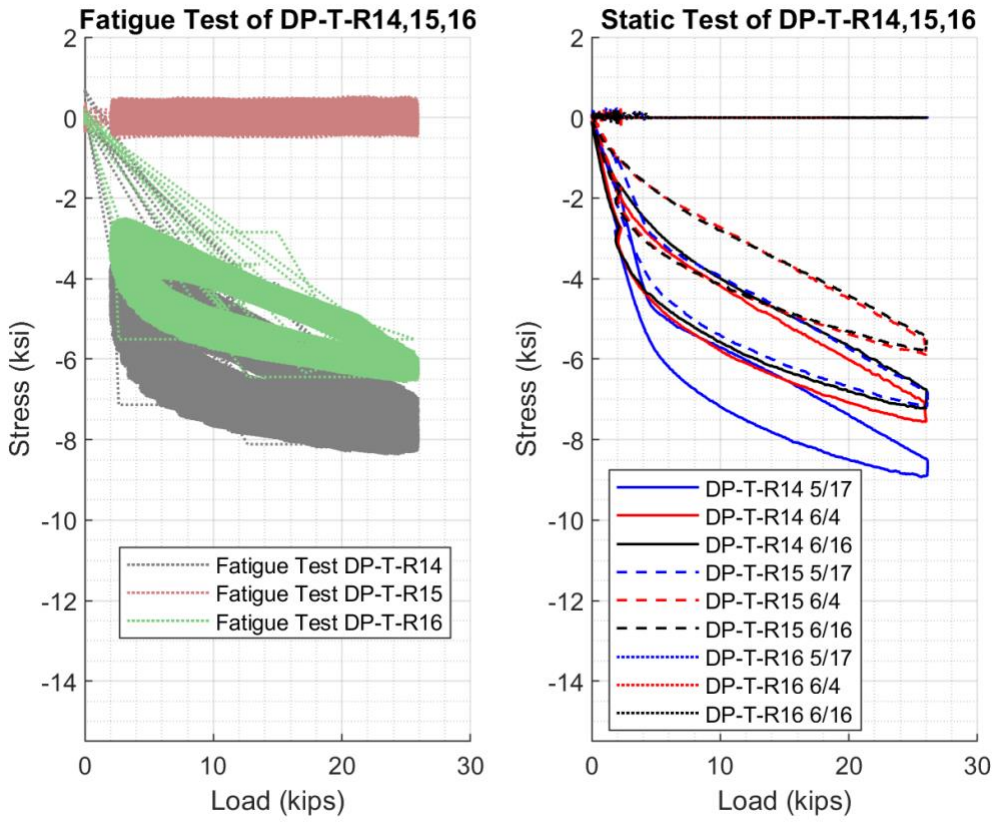

Figure 22 Fatigue and static test results of DP_T_R14,15,16

The gauge DP_T_R14,15,16 exhibited a nonlinear hysteritic response across all three static tests, with a noticeable jump at the maximum load. This response could be due to damage to the gauge, as it was located directly beneath the loading pad. The jump at the maximum load could suggest a slip phenomenon occurring during the loading process. The presence of slip could account for the observed hysteresis as the deck was loaded and unloaded. This behavior was consistent as the gauge response dropped at the same load for all three static tests. A similar response of the gauge across all static testes would imply that the gauge was not damaged.

Figure 23 illustrates the responses of the gauge BP_B_R17,18,19, positioned beneath the second corrugation on the underside of the bottom plate. This gauge was installed in situ and accordingly was not disturbed by the fabrication process. Arm R17 was aligned longitudinally along the deck, while the arm R19 was oriented transversely. Arm R18 was situated diagonally between R17 and R19.

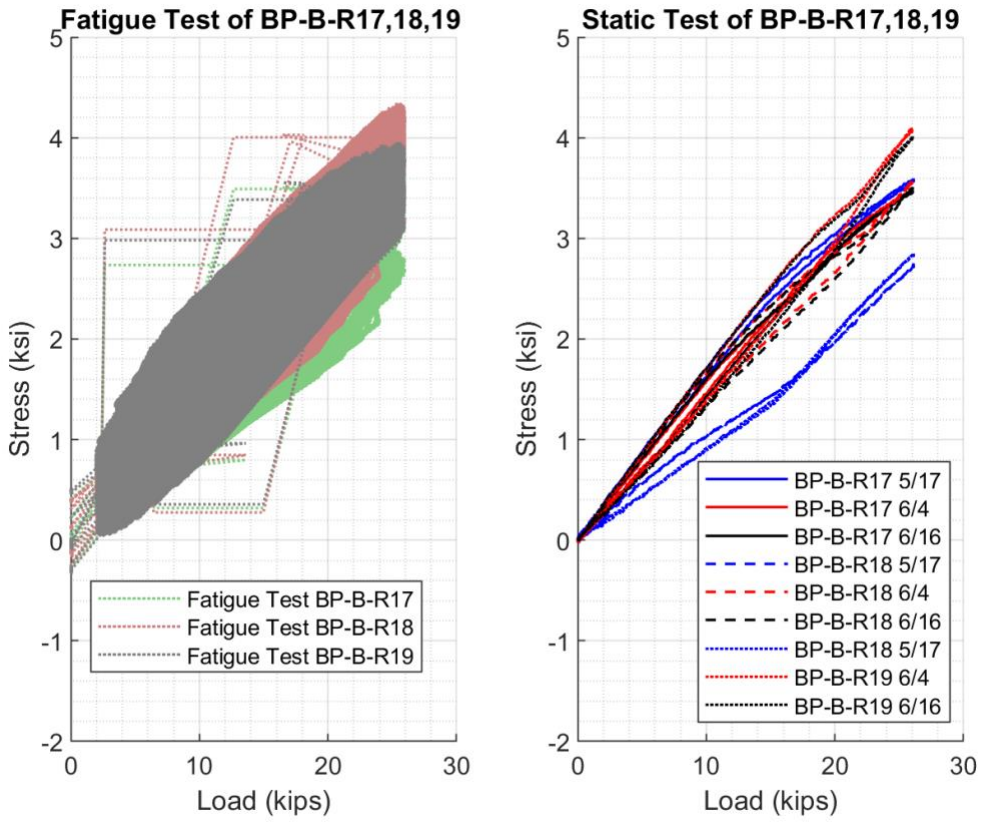

Figure 23 Fatigue and static test results of BP_B_R17,18,19

The results depicted in the graph exhibit a linear response, without any notable variation among the tests. The stress in the transverse direction during the first test was slightly lower than the other two tests, although the difference was not significant. Unlike the gauges located near adhesive connections, this particular gauge was positioned beneath a welded connection, which likely remained unaffected by the fatigue testing. The increase in the gauge response between the initial and subsequent static tests was likely due to the degradation of the adhesive connections at the deck plate, rather than the adjacent welded connection.

3.4. Measurements by the LVDTs

Three LVDTs were positioned beneath the deck that were exclusively employed during the static tests. The measurements from these LVDTs exhibited similar patterns. An increase of approximately 0.01 mils in displacement was observed between the initial and the subsequent tests. Ideally, the LVDT-measured displacement should be the loading divided by the deck stiffness. As the loading remained constant while the displacement increased, the stiffness of the deck specimen must have decreased between 5/17 and 6/4. This reduction in stiffness could be attributed to the deterioration of the adhesive connections between the core and the deck plate. The degradation of these adhesive connections would lead to a decline in the transverse flexural stiffness of the deck, causing an increase in vertical displacement. Figure 24, Figure 25, and Figure 26 showed the response of the three LVDTs.

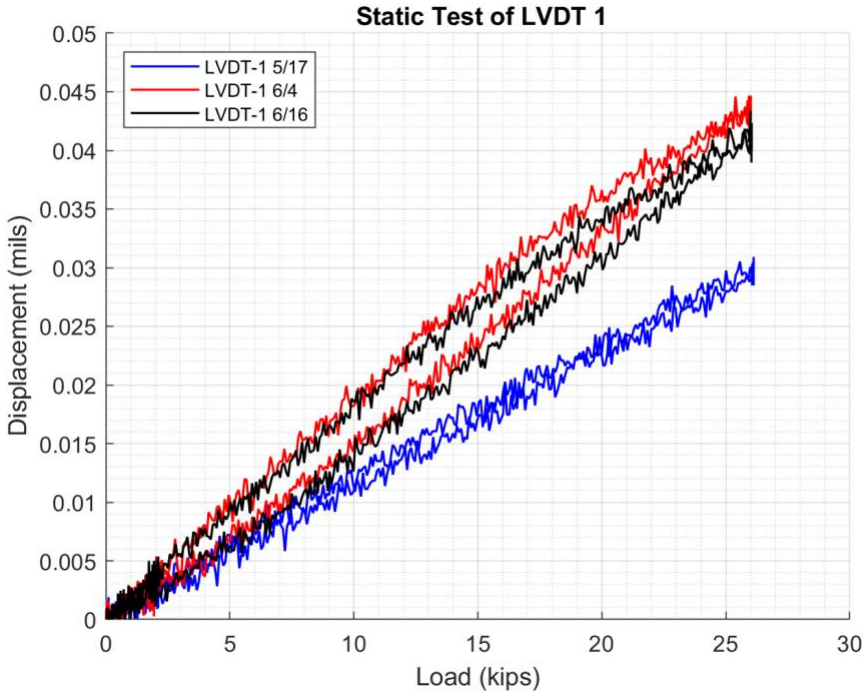

Figure 24 Static test results of LVDT 1

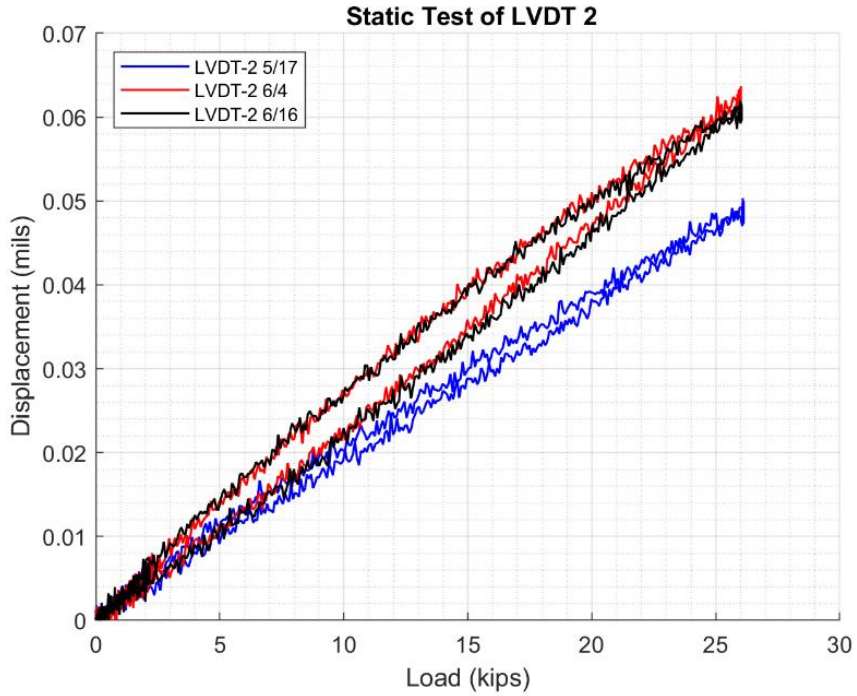

Figure 25 Static test results of LVDT 2

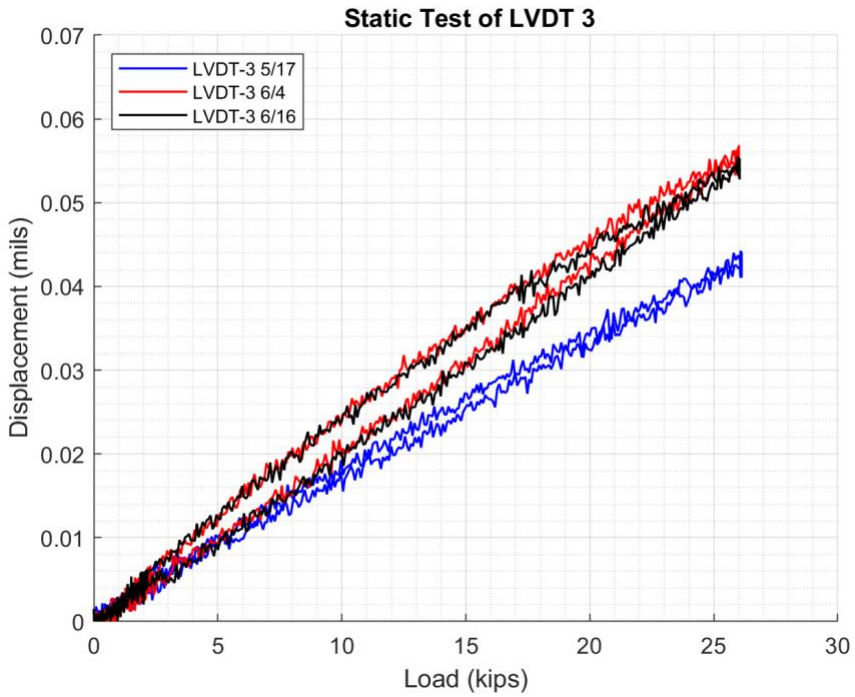

Figure 26 Static test results of LVDT 3

4. CONCLUSIONS

The performance of a steel sandwich plate bridge deck was evaluated by testing in the laboratory. The novelty of the deck was that the corrugated core was connected to the deck plate by structural adhesive. The deck was fatigue tested up to 5 million cycles subject to a 24 kip load range on a 10" × 20" simulated tire contact area at the middle of the deck. The load range exceeded the AASHTO HL93 fatigue limit state load. Throughout the testing process, the deck specimen exhibited changes in its state, as indicated by the results of the initial and intermittent static tests conducted. There was evidence of deterioration in the adhesive connection between the deck plate and the corrugated core. This was manifested by an increase in vertical displacement or a decrease in deck stiffness. The suspected deterioration influenced the load distribution, particularly in the transverse or primary span direction of the deck, leading to variations in stress measurements, as observed in the data. Some strain gauges showed signs of slipping, indicated by hysteresis and/or abrupt jumps in responses, further emphasizing the impact of adhesive deterioration.

Nevertheless, the deck specimen successfully endured over 5 million cycles of loading, demonstrating its durability. Overall, the evaluation of the steel sandwich plate bridge deck through laboratory testing provided valuable insights into its performance and highlighted areas for further investigation and improvement.

The laboratory testing was successfully performed employing MTS actuators procured for this project. These actuators and the test setup constructed for this project provided opportunities for exploring and developing cost-effective bridge decks for improving durability and extending service life of the transportation infrastructure.

5. REFERENCES

1. Nemry, F., & Demirel, H. (2012). Impacts of Climate Change on Transport: A focus on road and rail transport infrastructures. *European Commission, Joint Research Centre (JRC), Institute for Prospective Technological Studies (IPTS)*.
2. Knox, E, Cowling, M, and Winkle, I. 1998. "Adhesively bonded steel corrugated core sandwich construction for marine applications." Marine Structures, Vol. 11, pages 185-204